Journal of the European Ceramic Society **16** (1996) 1309–1318

PII: S0955-2219(96)00059-3
0955-2219/96/$15.00

Synthesis and Characterization of Y_2O_3–ZrO_2 and Y_2O_3–CeO_2–ZrO_2 Precursor Powders

T. Settu & R. Gobinathan

Ceramic Technology Division, Department of Chemical Engineering, Alagappa College of Technology, Anna University, Madras-600 025, India

(Received 24 April 1995; revised version received 6 March 1996; accepted 14 March 1996)

Abstract

Thixotropic gels of the precursor powders of the titled compounds have been prepared by the addition of oxalic acid to the mixed solutions of metal salts at room temperature (≈27°C). The clear sols of yttrium–zirconyl oxalate (YZO) and yttrium–cerium–zirconyl oxalate (YCZO) gelled within a few hours and were oven-dried at 40°C. The various stages of gelation behaviour of the sols are explained on the basis of DLVO theory. By repeptizing the dried gel powders with water, concentrated sols were prepared. The gelation time as a function of chloride ion concentration is discussed for both sols. The nature of the temperature dependence of the dried gel powders was studied by means of thermogravimetric analysis and differential thermal analysis. Powder X-ray diffraction was used to study the crystallization behaviour of the dried amorphous gel powders. It is found that these powders crystallize in tetragonal phase when calcined at 850°C for 1 h. Estimation of surface area and infra-red characterization have also been carried out for the prepared powders. © 1996 Elsevier Science Limited

1 Introduction

With the increasing development of ceramic materials, there has been enormous interest in their preparation. The preparation technique depends on the applications of a particular material, such as the mixed oxide method for refractory applications and chemical routes for structural and functional applications. The development of zirconia-based ceramic materials is of prime interest because of their superior properties such as toughness, oxidation, corrosion and erosion resistance and tolerance to severe environments, which enables numerous industrial applications. The pioneering work of Garvie *et al.*[1] and Gupta and co-workers[2,3] stimulated considerable attention on this area.

Although various liquid precursor routes are available for the preparation of fine ceramic materials, the sol–gel method is a promising processing technique because of its inherent advantages such as controlled particle size, shape and distribution, desired composition, relatively low-temperature sinterability, etc., and because of its recent advancement for industrial applications.[4–6]

Many reports on the preparation of fine particles of yttria-stabilized zirconia are available, several of which involved precipitation/sol–gel methods.[7–13] Most of them yielded sinteractive powders of fine size. The spray pyrolysis method has been used by Xiaming *et al.*[14] for the preparation of ZrO_2–Y_2O_3 powders.

Even though yttria-stabilized tetragonal zirconia has good mechanical properties, it suffers severely from low-temperature degradation[15–20] which leads to deleterious properties, and therefore the material turns out to be a failure. On the other hand, yttria–ceria-stabilized tetragonal zirconia has not shown low-temperature degradation.[20,21]

Many reports are available on the preparation of yttria–ceria-stabilized zirconia (YCZ) and its characterization.[19–22] Duh *et al.*[20] and Leach and Khan[22] have reported the mechanical behaviour, tolerance of the material in a hostile environment and the good phase stability of the YCZ system. The phase stability and mechanical behaviour of the stabilized zirconia are clearly explained by Hirano.[23]

The present work reports on the preparation of yttria- and yttria–ceria-stabilized zirconia by oxalate gelation using metal salts of chloride and nitrate, and oxalic acid solutions. The characterization of the prepared powders [by X-ray powder diffraction (XRD), thermogravimetric analysis (TGA), differential thermal analysis (DTA), surface area measurement and infra-red spectroscopy (IR)] and the preparation of concentrated sols are also discussed.

2 Experimental Procedure

The parent materials for the preparation of the titled powders were the water-soluble salts of metal nitrates and chlorides such as zirconyl chloride octahydrate (LR grade, CDH Chemicals), cerium nitrate hexahydrate (AR grade, CDH Chemicals), yttrium nitrate hexahydrate (AR grade, CDH Chemicals) and oxalic acid dihydrate (SD Fine Chemicals). Triple distilled water was used throughout the experiments. All the solutions were used as-prepared after filtration.

2.1 Preparation of gels

2.1.1 Yttrium–zirconyl oxalate (YZO) gel

Aqueous solutions (1 M) of zirconyl chloride and yttrium nitrate were prepared by dissolving the respective salts in water, and the solutions then thoroughly mixed together (corresponding to 5 mol% of Y_2O_3 in the final oxide powder). A desired amount of oxalic acid solution (1 M) was slowly added to the mixed cation solution with continuous stirring. White gelatinous precipitates were formed immediately, and gave a thick gel. The formed thick gel was vigorously stirred/shaken, yielding a clear sol. This sol was allowed to form a clear thixotropic gel at room temperature (≈27°C) by physical gelation. The addition of a stoichiometric ratio of oxalic acid led to the formation of a turbid aggregated sol. The physical and thixotropic gel obtained from the clear sol was oven-dried at 40°C. The dried gel powder has repeptizable character when mixed with water.

2.1.2 Yttrium–cerium–zirconyl oxalate (YCZO) gel

Solutions (1 M) of zirconyl chloride, cerium nitrate and yttrium nitrate were prepared by dissolving the salts in water. Cerium nitrate solution was first mixed well with zirconyl chloride solution and then the yttrium nitrate solution was thoroughly mixed with the combined solutions (corresponding to 4 mol% of Y_2O_3 and 7 mol% of CeO_2 in the final oxide powder). An appropriate quantity of oxalic acid solution (1 M) was mixed with the combined cation solution, slowly and with continuous stirring, at room temperature (≈27°C). During the formation of sol and gel, the observed characteristics of the YCZO system were the same as those of the YZO system. The prepared gels were oven-dried at 40°C and crushed in a mortar and pestle. The powders thus obtained were used to study the gelation time as a function of chloride ion concentration for repeptized sol. They were also calcined at different temperatures, 460, 600 and 850°C for 1 h, to study the crystallization behaviour and to estimate the surface area. Thermal behaviour and IR studies of the dried gel powders were also carried out.

The following flow chart shows the experimental procedure for the preparation of these powders.

Oxalic acid solution
↓
*Solutions of yttrium nitrate and zirconyl chloride
↓
White flocculation
↓
Clear sol
↓
Physical gelation
↓
Dried at 40°C
↓
Powder
↓
Characterization

*For the preparation of YCZO gel, cerium nitrate solution was mixed with the yttrium nitrate and zirconyl chloride solutions.

3 Results and Discussion

3.1 Formation of gels

Immediately after the oxalic acid solution is mixed with the combined solutions of yttrium nitrate and zirconyl chloride at room temperature (27°C), white flocculates are formed due to the localized concentration of the ions and the flocculates disappear spontaneously. If the addition of oxalic acid is continued, the rate of disappearance of the flocculates decreases and finally a white thick gel is obtained. After vigorous stirring/shaking of the gel, a clear sol is formed. Possible reasons for the variation of the rate of disappearance of the flocculates may be the higher ionic concentration of the solution and an uneven distribution of the ions. Vigorous stirring/shaking favours the even distribution of the ions and the adsorption of protons on the colloidal particles, thereby creating an electrical double layer. As time increases the clarity of the sol decreases slightly, which may be due to clustering of the colloidal particles. It has also been noticed that the atmospheric conditions have a marked effect on the formation of the transparent sol, gel and gelation time. For example, if the humidity of the atmosphere is greater than 95%, the formed sol and gel are highly transparent at room temperature and the time taken for

gelation is more; if the humidity is less than 90%, the formed sol is of aggregative nature and the gel is opaque. This may be due to the difference in the reaction rates for the formation of the sol and gel. However, a systematic study needs to be carried out to understand the effect of atmospheric conditions on sol and gel formation.

The YCZO gel was prepared by slow addition of oxalic acid to the combined cations solution with continuous stirring. The characteristics observed for this gel during preparation are similar to those of the YZO gel. The addition of a stoichiometric ratio of oxalic acid to the mixed cations solution leads to the formation of an unclear sol which then turns out to be a white opaque gel, whereas a transparent sol and gel are observed when the addition of oxalic acid is sufficient to form the zirconyl oxalate gel alone, i.e. the molar ratio of $(ZrO)^{2+}$ to $(C_2O_4)^{2-}$ is equal to 1 M for both YZO and YCZO gels. However, the time taken for the formation of the clear YCZO sol is less than that taken to form the YZO sol. Moreover, the transparency is higher for the YCZO than for the YZO system.

The cerium and yttrium ions are mixed in the form of their respective nitrate salts. The nature of the dopants in the zirconyl oxalate gel structure is not clearly understood. As Tohge *et al.*[24] suggested for glasses, here also we can think of the dopants as being uniformly distributed on the pore surface of the zirconyl gel structure; during calcination the dopant ions are substituted for zirconium ions in the crystal structure which favours the formation of the stabilized zirconia.

Although many forces are active in the solutions,[25] a possible qualitative explanation for the disappearance of the white flocculates at the beginning stage, the formation of the white thick gel at the middle stage and the clear sol at the final stage can be given by means of DLVO theory based on Refs 25 and 26. Conveniently, the existence of these three stages may be classified as follows: (1) the initial stage where the formed white flocculates disappear immediately after the oxalic acid is added to the mixed salt solutions; (2) the intermediate stage where the continued addition of oxalic acid to the combined solution of salts gives white flocculates which, instead of disappearing, lead to the formation of a white thick gel; and (3) the final stage where the observed white thick gel is slowly transformed to a clear transparent sol by continuously stirring/shaking.

It may be considered that the hydrochloric acid formed according to the following equation, which is for the preparation of pure zirconyl oxalate gel,[27] is one of the reasons for the coagulation and formation of the thick gel:

$$ZrOCl_2 + H_2C_2O_4 \rightarrow ZrOC_2O_4 + 2HCl \quad (1)$$

According to the DLVO theory, a potential energy barrier exists between two colloidal particles. Depending on the magnitude of the barrier, particles may be either coagulated or dispersed. The total potential energy of the interaction between two particles can be described by:

$$V_t = \frac{-\chi r}{12H} + 2\pi\epsilon r\psi_0^2 \exp(-\kappa H) \quad (2)$$

where H = inter-particle separation, ϵ = dielectric permitivity of the liquid medium, ψ_0 = surface potential and κ = Debye–Huckel parameter, given by

$$\kappa = ez\sqrt{\frac{n}{KT\epsilon}}$$

with K = Boltzmann constant, T = temperature, e = charge of an electron, z = number of charges on a particle and n = number of particles per unit volume.

From eqn (2), the energy barrier, V_b, can be derived as:

$$V_b = \frac{-\chi\kappa r}{12} + 2\pi\epsilon r\psi_0^2 \quad (3)$$

where r = particle diameter and χ = Hamaker constant. From eqn (3) it is clear that the energy

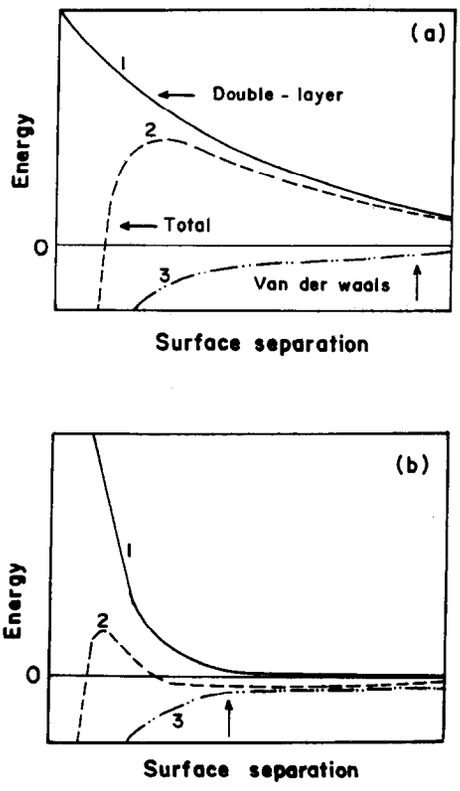

Fig. 1. Schematic plots of the energy of interaction between two surfaces across a polar liquid. Electrical double-layer repulsion gives a positive contribution which decreases exponentially as surface separation increases (line 1); van der Waals' attraction gives a negative term which is an inverse power-law function of separation (line 3). The net energy (line 2) is given by the sum of these two.[25]

barrier decreases when the dielectric constant of the medium decreases. When the oxalic acid is added to the mixed aqueous solutions of zirconyl chloride and yttrium or cerium nitrate, the dielectric constant of the total system may be decreased due to the formation of hydrochloric acid, so that the formed white flocculates disappear immediately. This may be due to the thickness of the electrical double layer, which is explained on the basis of Fig. 1.

As shown in Fig. 1(a), at low electrolytic concentration the double-layer term dominates at large separations, giving a maximum in the energy. The height of this energy barrier depends on the surface charge density and the electrolyte concentration. On the basis of the reaction it is clear that 2 moles of hydrochloric acid are formed for the addition of 1 mole of oxalic acid with zirconyl chloride. Considering the entire solution system, at the beginning stage, the addition of a small amount of oxalic acid to zirconyl chloride gives only a small amount of hydrochloric acid. This may result in a very small decrease in the dielectric constant and hence the formed flocculates disappear.

As the addition of oxalic acid to zirconyl chloride solution continues, more hydrochloric acid is formed which causes a further decrease in the dielectric constant of the system. Although the like ionic repulsion is more, the particles collide with sufficient kinetic energy which is greater than the repulsion and hence they can stick together to give thick colloidal gel. Similar observations have been reported by Li and Messing[28] in the preparation of spherical zirconia particles.

It can be seen from Fig. 1(b) that, at higher concentrations, the double-layer term may decay so rapidly that the van der Waals' attraction is still significant at a separation beyond the range of the repulsion, and the particles can reside in a secondary minimum [arrow in Fig. 1(b)]. This gives a much weaker attraction, which could easily be overcome by shear. According to this, if the formed gel is continuously stirred/shaken, the thick-white gel will slowly disappear and give a clear sol.

3.2 Crystallization behaviour

To study the crystalline nature of the prepared dried gel powders and calcined powders, X-ray diffraction analysis has been carried out. Figures 2 and 3 show the XRD patterns for the dried and calcined powders of YZO and YCZO gels, respectively, calcined at different temperatures for 1 h. Both powders, dried at 40°C, are amorphous. At 460°C, the powders start to crystallize in tetragonal phase. For calcination temperatures of 600°C and above, retention of the tetragonal phase has been observed for both systems. The increased crystallite size is reflected in Figs 2 and 3 as the decrease in the width of the spectral lines.

To identify whether the formed phase is tetragonal or cubic, higher-angle XRD patterns (insert in Figs 2 and 3) have been recorded for both powders calcined at 850°C for 1 h. From the insert in the figures, it is observed that both tetragonal and cubic phases are present. These are identified from the reflections $(0\,0\,4)_t$, $(0\,0\,4)_c$ and $(4\,0\,0)_t$.

3.3 Thermal analysis

TGA and DTA studies were carried out to analyse the weight loss and phase transition behaviour of the dried YZO and YCZO gels (for all curves, heating rate = 10°C min^{-1} and atmosphere = air). Figure 4 shows the TGA curve for the dried YZO gel powder in the temperature range 30 to 800°C. It can be observed that there are three major weight losses of 17·91, 12·22 and 19·74%. The first weight loss corresponds to the removal of water

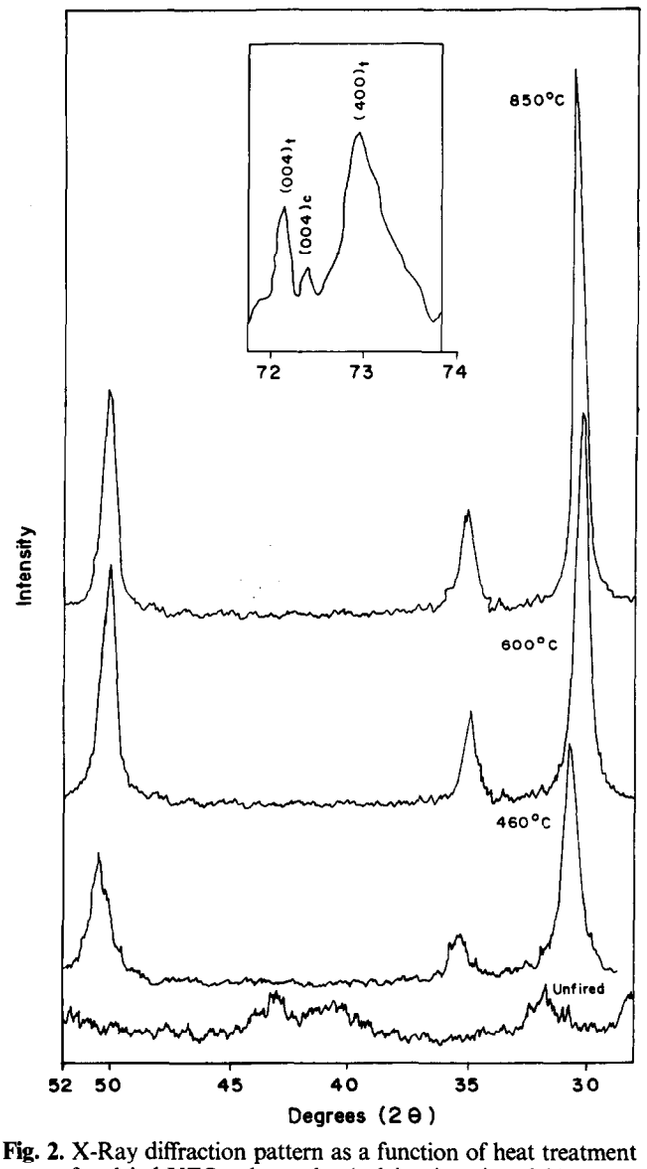

Fig. 2. X-Ray diffraction pattern as a function of heat treatment for dried YZO gel powder (calcination time 1 h).

and the next one is due to the decomposition of the nitrate. The last weight loss may be due to the decomposition of oxalate with the simultaneous formation of amorphous and tetragonal zirconia powder. Two more weight losses of 1·48 and 2·80% have also been observed. These losses may be due to the liberation of adsorbed/occluded chlorides in the dried gel powder.

Figure 5 shows the DTA curve of the dried YZO gel powder, in which two endothermic and an exothermic peaks are observed. The endothermic peak around 170°C is due to the removal of adsorbed water as observed in the TGA curve. A small endothermic peak around 250°C is observed which may be due to the removal of structural hydroxyl groups, and is not resolved even in the DTG curve. The existence and removal of the hydroxyl group has been confirmed by IR spectra for the samples collected at their peak temperatures, 170 and 250°C, respectively. The decomposition of nitrate has not been well resolved in the DTA curve. The shoulder around 285°C in the second broad endothermic peak may be due to the decomposition of nitrates, which is clearly identified in the TGA curve. The endothermic peak around 345°C may be attributed to the decomposition of oxalate as observed in the TGA curve. The oxalate decomposition step starts before complete decomposition of the nitrate. The exothermic peak around 467°C is due to the crystallization of amorphous oxide powder in tetragonal phase.

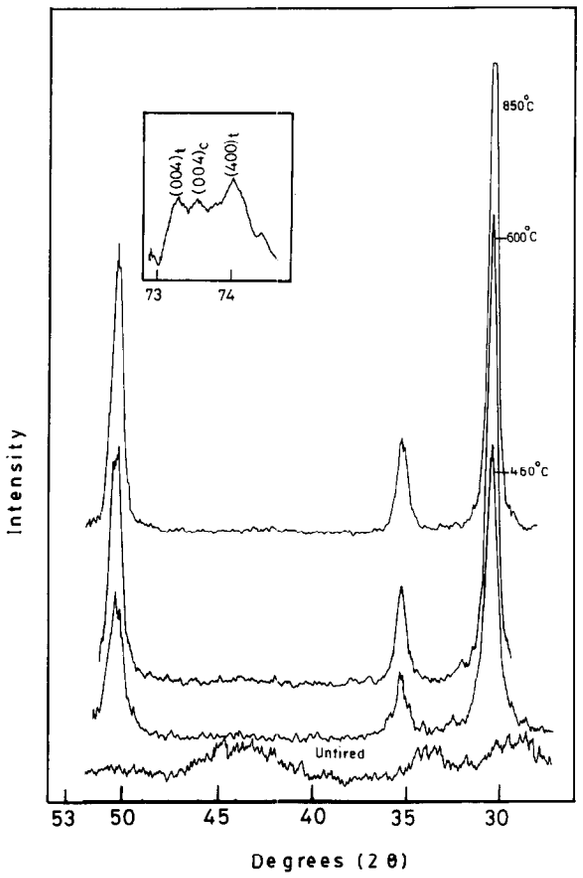

Fig. 3. X-ray diffraction pattern as a function of heat treatment for dried YCZO gel powder (calcination time 1 h).

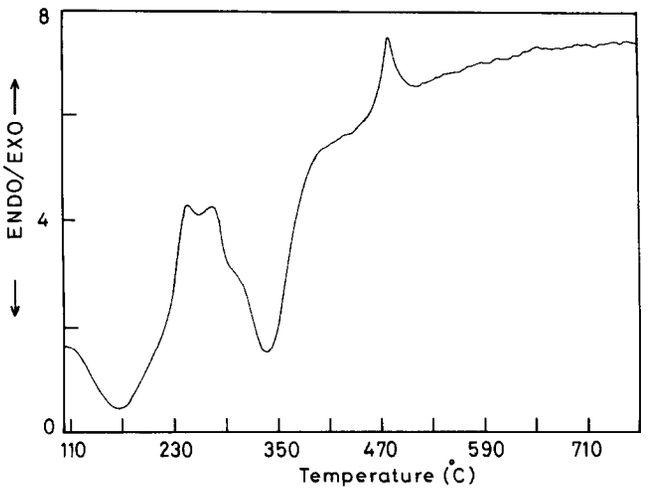

Fig. 5. DTA curve for the YZO gel powder dried at 40°C.

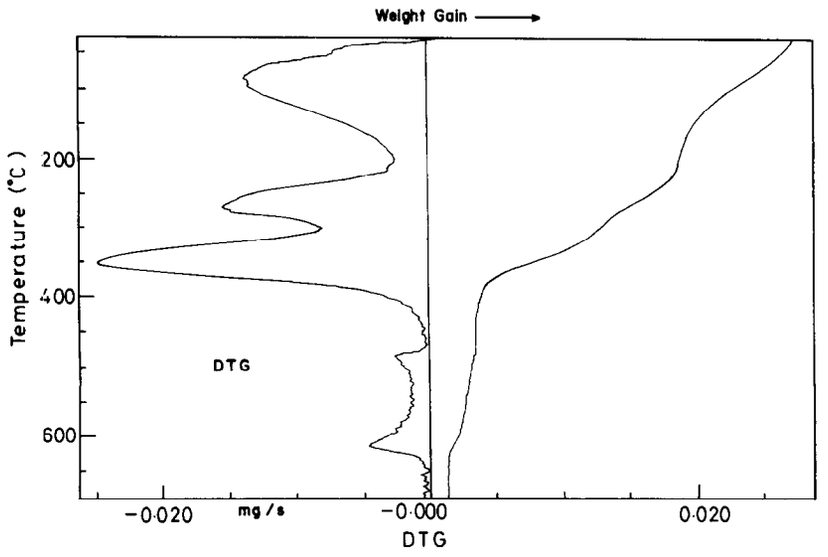

Fig. 4. TGA curve for the YZO gel powder dried at 40°C.

This is confirmed by the X-ray diffractogram (Fig. 2) for the sample that has been isothermally heat-treated at 460°C for 1 h. The liberation of chlorides has not been observed in the DTA curve, which may be due to the smooth release of the same.

From the TGA curve (Fig. 6) of the dried YCZO gel powders, it is clear that there are three major weight losses of 18·83, 17·64 and 12·9%. The first is due to the removal of adsorbed water and the second corresponds to the decomposition of nitrate. The third weight loss may be due to the decomposition of oxalate.

Although nitrate and oxalate decompositions seem to be single step, the oxalate step is actually a double decomposition. The first partial oxalate decomposition overlaps with the nitrate decomposition. This is not resolved by the TGA or the DTG curves. The second oxalate decomposition step occurred in the temperature range 289 to 462°C.

There are two more small weight losses observed in the temperature range 470 to 640°C. These may be attributed to the smooth release of adsorbed/occluded chloride and residual carbon dioxide, respectively.

It can be seen from Fig. 7, the DTA curve for the dried YCZO gel powder, that there are one endothermic and three exothermic peaks corresponding to

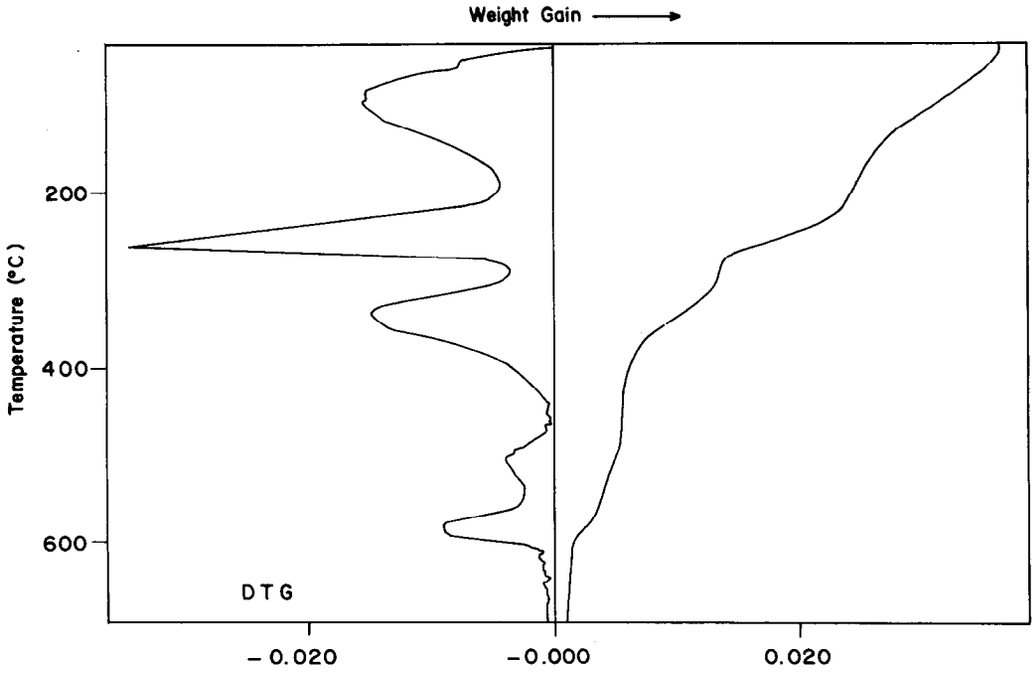

Fig. 6. TGA curve for the YCZO gel powder dried at 40°C.

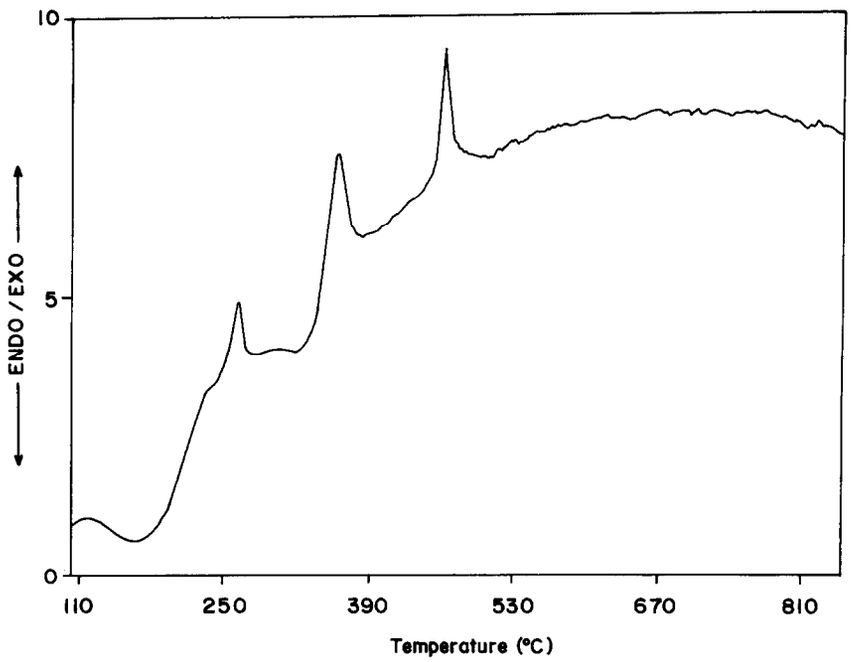

Fig. 7. DTA curve for the YCZO gel powder dried at 40°C.

temperatures around 170, 270, 340 and 470°C, respectively. The endothermic peak around 170°C is due to the removal of physisorbed water, as observed in the TGA curve. As observed in the TGA curve, the burning and release of nitrate occurred at around 270°C. The peak around 340°C may be attributed to the decomposition of oxalate, which has also been observed in the TGA curve. It can be seen that the decomposition of oxalate is not resolved by the DTA curve also. The exothermic peak around 470°C is due to the crystallization of amorphous YCZO powder in tetragonal phase with the simultaneous release of chlorides. The formation of tetragonal phase has clearly been confirmed by the X-ray diffraction patterns (Fig. 3) for the sample which was isothermally heat-treated at 460°C for 1 h. The liberation of chloride and carbon dioxide has not been observed explicitly in the DTA curve.

It is quite interesting to note that all the decomposition steps, for the dried YCZO gel powder, are exothermic in nature (except for water removal) whereas endothermic peaks have been observed for the dried YZO gel powder. The observed difference in the decomposition nature of these compounds lies in the presence of cerium ions. In our previous work.[29] we reported the exothermic decomposition of ceria–zirconia amorphous precursor powders. Accordingly, during the decomposition step, Ce^{3+} ions oxidize to Ce^{4+} ions. By considering the ionic radius, the possibility of substitution of the Ce^{3+} ions into the ZrO_2 crystal structure is highly remote at low temperatures and hence the only chance is the formation of Ce^{4+} ions due to the oxidation of Ce^{3+} ions. These Ce^{4+} ions substitute for Zr^{4+} ions in the ZrO_2 crystal structure and favour the formation of tetragonal solid solution. However, in reducing atmospheres at temperatures above 1200°C, the formation of $Ce_2Zr_2O_7$ has also been reported.[30] But the X-ray diffraction patterns (Fig. 3) do not show the existence of Ce_2O_3 reflections. This shows, conclusively, that the observed exothermic peaks are due to the exothermic oxidation of dried YCZO gel powder.

3.4 Preparation of concentrated sol

The preparation method of sol 1 (for both YZO and YCZO) has been clearly discussed in an earlier section. The gel that was formed by the gelation of sol 1 was oven-dried at 40°C. The gel powder obtained from the dried gel was slowly added to water with continuous stirring. The powder slowly dissolved in water giving a more clear sol, namely sol 2, than sol 1. The quantity of water taken for the preparation of sol 2 is the same as that for sol 1. This process was repeated a number of times. As given in eqn (1), the hydrochloric acid formed during the reaction of the reactants plays an important role for the repeptization of the dried gel powder and the formation of a more clear gel by sol 2. Along with the chloride ions the nitrate ions are also responsible for the repeptization of the dried gel powder. The adsorption of the positive charges on the surfaces of the particles may be the reason for the repeptization of the dried gel powder. The different stages of the gelation and cycling processes are given in the following chart.

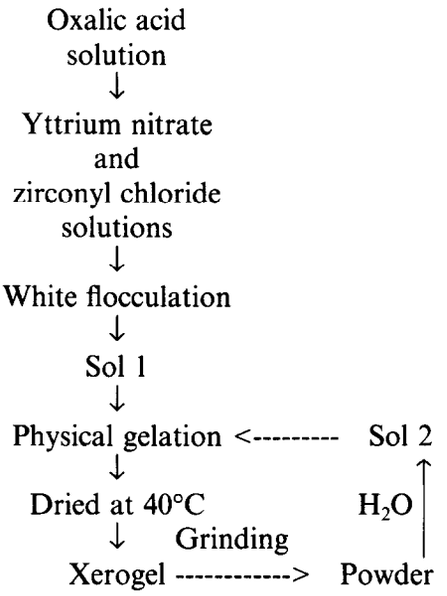

The gelation time as a function of chloride ion concentration for sol 1 and sol 2 is shown

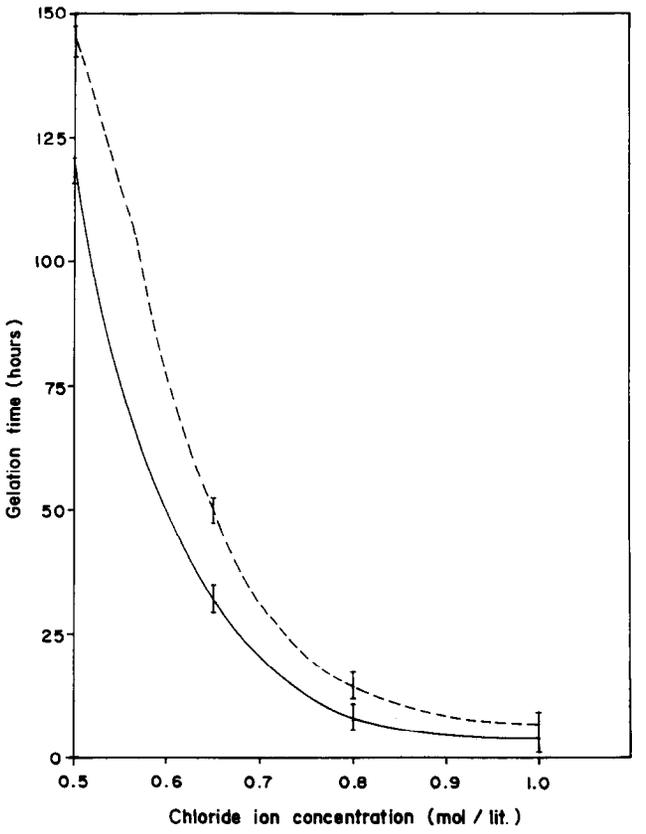

Fig. 8. Gelation time as a function of concentration of chloride ion for sol 1 —, YZO system; – – –, YCZO system.

in Figs 8 and 9, respectively. It is found that, for sol 1, the gelation time has exponential character with the concentration of the chloride ion whereas for sol 2 the character is linear. As the concentration of the oxide powder (chloride ion) increases, the gelation time decreases. The concentration of the chloride ions in sol 2 has been estimated using Volhard's volumetric method. The gelation time has been calculated as the time taken from the formation of the clear sol to the gelation point. The approximate gelation point was that time at which the semi-rigid mass did not come out of the beaker while tilting it.

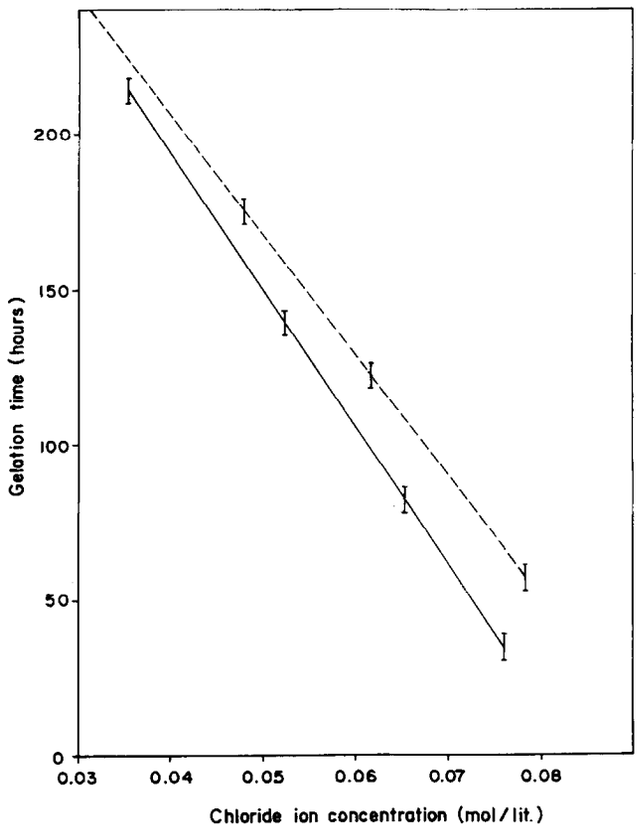

Fig. 9. Gelation time as a function of concentration of chloride ion for sol 2 —, YZO system; – – –, YCZO system.

It is possible to increase the concentration of the oxide powder in the sol using the dried gel powders. Sol 1 of YZO and YCZO contains 5·81 wt% and 6·17 wt% of their respective oxide powders. For the same wt% of the respective powders, the gelation time for the repeptized sol 2 is higher than that of sol 1. This may be due to removal of the excess of hydrochloric acid that was formed during reaction of the reactants. It has been observed that the wt% of the oxide powder can be increased up to 10 wt% for the YCZO powder in sol 2, whereas the wt% of YZO in sol 2 cannot be increased because of its highly viscous nature. There is a difference in gelation times observed for sol 2 of YZO and YCZO. This may be due to the observed difference in the viscous nature of their respective repeptized sols.

Viscosimetric studies were carried out to study the viscous nature of the sols. Immediately after the formation of clear sol 1, the observed viscosity is almost the same as that of water. The viscosity is approximately 16000 mPa s after 15 min for sol 1 of YZO, whereas for sol 1 of YCZO the same value of viscosity is observed after 40 min. However, as observed for sol 1, the rate of increase of viscosity is more for sol 2 of YZO than for sol 2 of the YCZO system.

The large difference observed in gelation time for sols 1 and 2 arises from the total concentration of ions. In the repeptized sol, due to removal

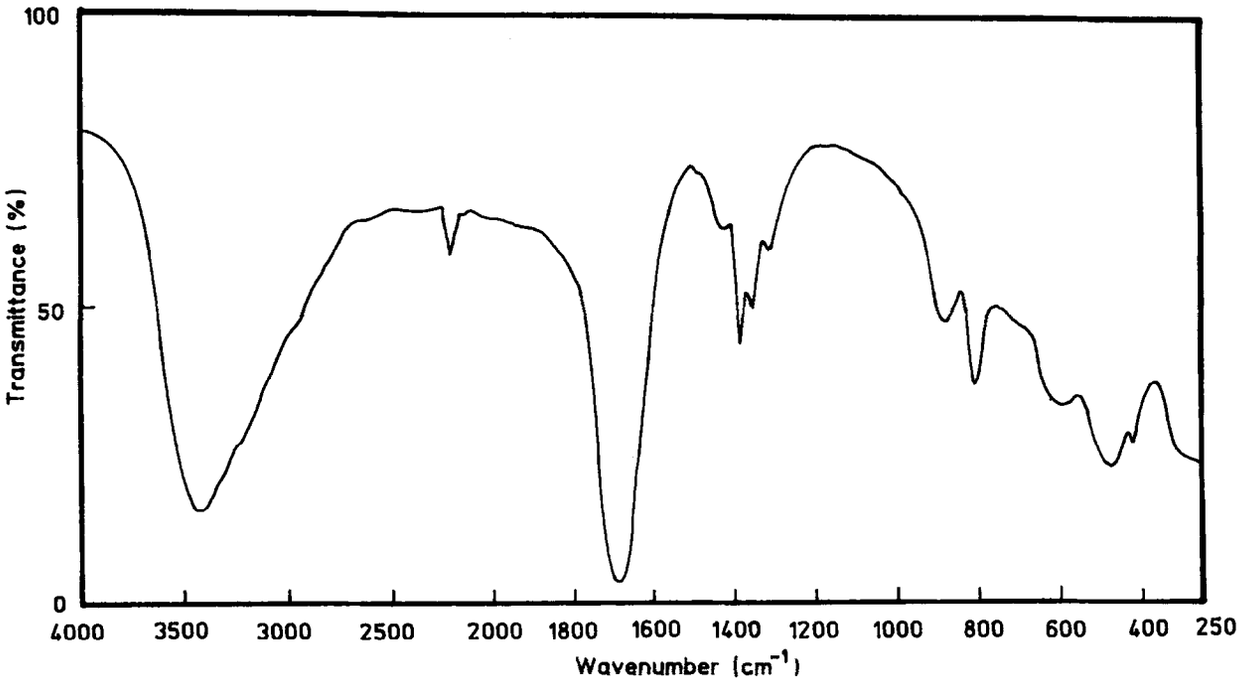

Fig. 10. IR spectrum for the YZO gel powder dried at 40°C.

of the excess hydrochloric acid during drying, the total concentration of ions in sol 2 is reduced and hence the thickness of the electrical double layer is increased.

3.5 IR characterization

Figures 10 and 11 show the IR spectra for the YZO and YCZO powders dried at 40°C. It has been reported that the oxalate ion has a quadridentate structure with the zirconium ion.[27] It seems that the addition of yttrium and cerium ions as their nitrates does not affect the structure of the zirconyl oxalate. Compared with our earlier results,[29] the appearance of the peak at 1390 cm^{-1} is due to the presence of nitrates in the dried oxalate gel powder. On calcination of the dried gel powders, the removal of water and decomposition of nitrate and oxalate are observed, as indicated from the TGA and DTA results. As mentioned before in the DTA results of the dried YZO gel powder, the small peak around 250°C is due to the removal of the hydroxyl group as confirmed from the IR spectrum taken for the sample collected at this peak temperature. Table 1 shows the vibrational frequencies of the dried powders of the YZO and YCZO gels.

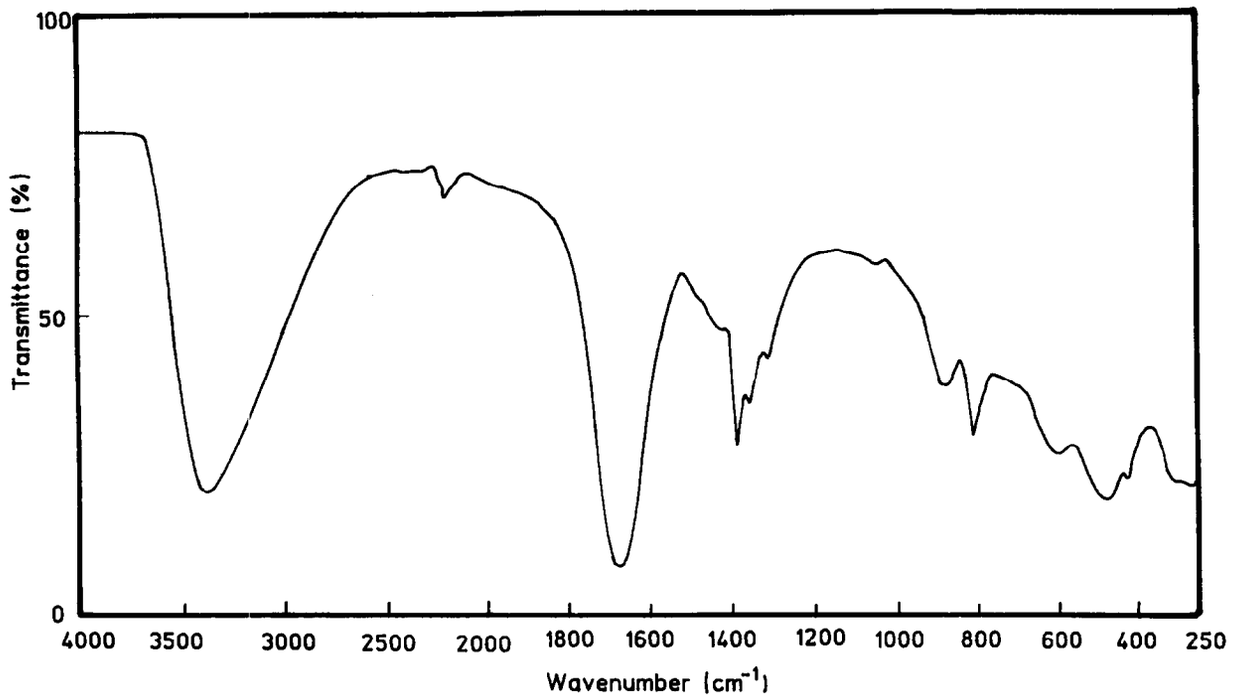

Fig. 11. IR spectrum for the YCZO gel powder dried at 40°C.

Table 1. Assignment of IR bands

Vibrational frequency (cm^{-1})			*Group*
CZO[a] (Ref. 29)	*YZO*	*YCZO*	
1680	1670	1670	ν_{as} (C=O)
1425	1420	1420	ν_s (C–O) + ν (C–C)
1390	1380	1835	$(NO_3)^-$
1355	1350	1355	ν_s (C–O) + δ (O–C=O)
900	880	885	ν_s (C–O) + δ (O–C=O)
815	805	805	ν(Zr–O) + δ (O–C=O)
480	470	475	(Zr–O–Zr)

[a] CZO is the cerium–zirconyl oxalate dried gel powder.

Table 2. Variation of surface area as a function of temperature, measured by BET technique

	YZO			*YCZO*		
Firing temperature (°C)	460	600	850	460	600	850
Specific area ($m^2 g^{-1}$)	34	23	5	35	27	6
Average crystallite size (nm)	24	32	112	23	27	114

3.6 Surface area measurement

Specific surface area has been estimated for the YZO and YCZO powders using the BET technique with nitrogen. The dried gel powders were calcined at different temperatures such as 460, 600 and 850°C for 1 h. Assuming the prepared calcined powder particles to be spherical in shape, the average crystallite sizes of the powders have been calculated. From Table 2 it is found that the surface area of the calcined powders decreases as the calcination temperature increases, due to the increase of the crystallite size.

4 Conclusion

Transparent, physical and thixotropic YZO and YCZO gels have been prepared by oxalate

gelation. A possible explanation has been presented for the various stages of gel formation by means of DLVO theory. Because of the repeptizable character, it is possible to prepare concentrated sols. DTA studies show the YZO and YCZO dried amorphous gel powders are crystallized in the tetragonal phase around 470°C. This has been confirmed by powder X-ray diffraction studies. These amorphous dried gel powders may be useful for the preparation of the fine tetragonal zirconia polycrystalline powders.

Acknowledgements

The authors acknowledge the interest shown by Professor F. D. Gnanam, Alagappa College of Technology, Anna University, Professor T. Nagarajan, Head, and thank Dr V. Sridharan, Department of Nuclear Physics, University of Madras, for the thermal analysis experiments. One of the authors (T. S.) thanks the Council of Scientific and Industrial Research, Government of India for providing a fellowship to carry out this work.

References

1. Garvie, R. C., Hannink, R. H. & Pascoe, R. T., Ceramic steel? *Nature*, **258** (1975) 703–5.
2. Gupta, T. K., Bechtold, R. C., Kuznicki, C. L. H. & Rossing, B. R., Stabilization of tetragonal phase in polycrystalline zirconia. *J. Mater. Sci.*, **12** (1977) 2421–6.
3. Gupta T. K., Lange F. F. & Bechtold, T. H., Effect of stress-induced phase transformation on the properties of polycrystalline zirconia containing metastable tetragonal phase. *J. Mater. Sci.*, **13** (1978) 1464–70.
4. Wenzel, J., Trends in sol–gel processing: toward 2004. *J. Non-Cryst. Solids*, **73** (1985) 693–9.
5. Dislich, H., Sol–gel: science, processes and product. *J. Non-Cryst. Solids*, **80** (1986) 115–21.
6. Wilson, G. & Heathcote, R., Role of sol–gel powders in thermal-spray process. *Bull. Am. Ceram. Soc.*, **69** (1990) 1137–9.
7. Mazdiyasni, K. S., Lynch, C. T. & Smith II, J. S., Cubic phase stabilization of translucent yttria–zirconia at very low temperature. *J. Am. Ceram. Soc.*, **50** (1967) 532–7.
8. Uchiyama, K., Ogihara, T., Ikemoto, T., Mizutani, N. & Kato, M., Preparation of monodispersed Y-doped ZrO_2 powders. *J. Mater. Sci.*, **22** (1987) 4343–7.
9. Aiken, B., Hsu, W. P. & Matijevic, E., Preparation and properties of uniform mixed and coated colloidal particles. *J.Mater. Sci.*, **25** (1990) 1886–94.
10. Groot Zevert, W. F. M., Winnubst, A. J. A., Theunissen, G. S. A. M. & Burggraaf, A. J., Powder preparation and compaction behaviour of fine-grained yttria doped tetragonal zirconia polycrystals (Y-TZP). *J. Mater. Sci.*, **25** (1990) 3449–55.
11. Wen, T. L., Hebert, V., Vilminot, S. & Bernier, J. C., Preparation of nanosized yttria-stabilized zirconia powders and their characterization. *J. Mater. Sci.*, **26** (1991) 3787–91.
12. Bourell, D. L., Parimal & Kaysser, W., Sol–gel synthesis of nanophase yttria-stabilized tetragonal zirconia and densification behavior below 1600 K. *J. Am. Ceram. Soc.*, **76** (1993) 705–11.
13. Samdi, A., Durand, B., Daoudi, A., Chassagneux, F., Deloume, J. P., Taha, M., Paletlo, J. & Fantozzi, G., Influence of formation pH and grinding of precursors on compaction and sintering behaviours of 3 mol% Y_2O_3–ZrO_2. *J. Eur. Ceram. Soc.*, **114** (1994) 131–41.
14. Xiaming, D., Qingfeng, L. & Yuying, T., Study of phase formation in spray pyrolysis of ZrO_2 and ZrO_2–Y_2O_3 powders. *J. Am. Ceram. Soc.*, **76** (1993) 760–2.
15. Kobayashi K., Kuwajima, H. & Masaki, T., Phase change and mechanical properties of ZrO_2–Y_2O_3 solid electrolyte after aging. *Solid State Ionics*, **3–4** (1981) 489–93.
16. Sato, T. & Shimada, M. Crystalline phase change in yttria partially stabilized zirconia by low temperature annealing. *J. Am. Ceram. Soc.*, **67** (1984) C212–3.
17. Sato, T. & Shimada, M., Transformation of yttria doped tetragonal ZrO_2 crystals by annealing in water. *J. Am. Ceram. Soc.*, **68** (1985) 356–9.
18. Sato T., Ohtaki, S. & Shimada, M., Transformation of yttria partially stabilized zirconia by low temperature annealing in air. *J. Mater. Sci.*, **20** (1985) 1466–70.
19. Hernandez, T. M., Jurado, R. J., Duran, P. & Fierro, J. L. G., Subeutectoid degradation of yttria-stabilized tetragonal zirconia polycrystal and ceria-doped yttria-stabilized tetragonal zirconia polycrystal ceramics. *J. Am. Ceram. Soc.*, **74** (1991) 1254–8.
20. Duh, J. G., Dai, H. T. & Chiou, S. B., Sintering, microstructure, hardness, and fracture toughness behaviour of Y_2O_3–CeO_2–ZrO_2. *J. Am. Ceram. Soc.*, **71** (1988) 813–19.
21. Tsukuma, K. & Shimada, M., Strength, fracture toughness and Vickers hardness of CeO_2-stabilized tetragonal ZrO_2 polycrystals (Ce-TZP). *J. Mater. Sci.*, **20** (1985) 1178–84.
22. Leach, C. & Khan, N., Stability of zirconia–ceria–yttria ceramics in hostile environments. *J. Mater. Sci.*, **26** (1991) 2026–30.
23. Hirano, M., Inhibition of low temperature degradation of tetragonal zirconia ceramics — a review. *Br. Ceram. Trans. J.*, **91** (1992) 147–50.
24. Tohge, N., Moore, G. S. & Mackenzie, J. D., Structural developments during the gel to glass transition. *J. Non-Cryst. Solids*, **63** (1984) 65–103.
25. Horn, R. G., Surface forces and their action in ceramic materials. *J. Am. Ceram. Soc.*, **73** (1990) 1117–35.
26. Pottel, R., in *Water — A Comprehensive Treatise*, Vol. 3, ed. Felix Franks. 1982.
27. Etienne, J., Larbot A., Guizard, C., Cot, L. & Alary, J. A., Preparation and characterization of zirconyl oxalate gel. *J. Non-Cryst. Solids*, **125** (1990) 224–9.
28. Li, M. & Messing, L., Preparation of spherical zirconia particles by controlled coagulation in zirconia sols. In *Ceramic Transactions Vol. 12, Ceramic Powder Science III*, eds L. Messsing & H. Hausner. *Am. Ceram. Soc.*, Westerville, OH, 1990.
29. Settu, T. & Gobinathan, R., Preparation and thermal evolution of sol–gel derived zirconia and ceria–zirconia precursors. *Bull. Chem. Soc. Jpn*, **67** (1994) 1999–2005.
30. Zhu, H. Y., Hirata, T. & Muramatsu, Y., Phase separation in 12 mol% ceria-doped zirconia induced by heat treatment in H_2 and Ar. *J. Am. Ceram. Soc.*, **75** (1992) 2843–8.